Upscaling of Transport Equations for Multiphase and Multicomponent Flows

Richard Ewing[1], Yalchin Efendiev[1], Victor Ginting[2], and Hong Wang[3]

1. Department of Mathematics and Institute for Scientific Computation, Texas A & M University, College Station, TX 77843-3404, USA, richard-ewing@tamu.edu, efendiev@math.tamu.edu
2. Department of Mathematics, Colorado State University, Fort Collins, CO 80523-1874, USA, ginting@math.colostate.edu
3. Department of Mathematics, University of South Carolina, Columbia, SC 29208, USA, hwang@math.sc.edu

Summary. In this paper we discuss upscaling of immiscible multiphase and miscible multicomponent flow and transport in heterogeneous porous media. The discussion presented in the paper summarizes the results of in *Upscaled Modeling in Multiphase Flow Applications* by Ginting et al. (2004) and in *Upscaling of Multiphase and Multicomponent Flow* by Ginting et al. (2006). Perturbation approaches are used to upscale the transport equation that has hyperbolic nature. Our numerical results show that these upscaling techniques give an improvement over the existing upscaled models which ignore the subgrid terms.

1 Introduction

The high degree of variability and multiscale nature of formation properties such as permeability pose significant challenges for subsurface flow modeling. Upscaling procedures are commonly applied to solve flow and transport equations in practice. On the fine (fully resolved) scale, the subsurface flow and transport of N components can be described in terms of an elliptic (for incompressible systems) pressure equation coupled to a sequence of $N-1$ hyperbolic (in the absence of dispersive and capillary pressure effects) conservation laws. Although there are various technical issues associated with subgrid models for the pressure equation, the lack of robustness of existing coarse scale models is largely due to the treatment of the hyperbolic transport equations. In this paper, we discuss the use of perturbation approaches for correcting the existing upscaled models for transport equations. Two-phase immiscible flow as well as miscible two-component flow are considered.

Previous approaches for the coarse scale modeling of transport in heterogeneous oil reservoirs include the use of pseudo relative permeabilities [2], the application of nonuniform or flow-based coarse grids [5], and the use of

volume averaging and higher moments [7, 6]. Our methodology for subgrid upscaling of the hyperbolic (or convection dominated) equations uses volume averaging techniques. In particular, a perturbation analysis is employed to derive the macrodispersion that represents the effects of subgrid heterogeneities. The macrodispersion, in particular, can be written as time integration of a covariance between the velocity fluctuations and fine scale quantity that represents the length of fine scale trajectories. For the computation of fine scale quantities, we use detailed information that is contained in multiscale basis functions. We note that the resulting macrodispersion depends on the saturation due to the functional dependence of the velocities on it. Thus, a mere use of this macro-dispersion model would require saving the velocities for each time. We discuss a procedure to overcome the aforementioned impracticality by proposing a recursive relation relating the length of fine scale trajectories to the velocities.

2 Fine and Coarse Models

In this section, we briefly present mathematical models for two-phase immiscible and two-component miscible flow and transport. Because of the similarities of the governing equations, we present both models using the same equations (with some abuse of notations):

$$\nabla \cdot v = q$$
$$S_t + v \cdot \nabla f(S) = (\tilde{S} - f(S))q, \quad v = -d(S)k(x)\nabla p, \tag{1}$$

where p is the pressure, S is the saturation (or concentration), $k(x)$ is a heterogeneous permeability field, v is the velocity field and q is the source term, and $\tilde{S}$ is the given saturation at the source term locations. The system is subject to some initial and boundary conditions. We will discuss upscaling techniques for (1). In further discussions, we refer to the first equation as the pressure equation (p is the pressure) and to the second equation as the saturation equation (S is the saturation or concentration).

For miscible two-component flow, $d(S) = \frac{1}{\mu(S)}$, where $\mu(S)$ is the viscosity function and has the form $\mu(S) = \frac{\mu(0)}{\left(1-S+M^{\frac{1}{4}}S\right)^4}$, and $f(S) = S$, where S is the concentration (will be referred as saturation in later discussions). For immiscible displacement of two-phase flow,

$$d(S) = \frac{k_{r1}(S)}{\mu_1} + \frac{k_{r2}(S)}{\mu_2}, \quad f(S) = \frac{k_{r1}(S)/\mu_1}{k_{r1}(S)/\mu_1 + k_{r2}(S)/\mu_2}. \tag{2}$$

Here $k_{ri}(S)$ ($i = 1, 2$) are relative permeabilities of phase i (e.g., water and oil), μ_i are viscosities of phase i.

Previous approaches for upscaling such systems are discussed by many authors; e.g., [1]. In most upscaling procedures, the coarse scale pressure equation

is of the same form as the fine scale equation, but with an equivalent grid block permeability tensor k^* replacing k. For a given coarse scale grid block, the tensor k^* is generally computed through the solution of the pressure equation over the local fine scale region corresponding to the particular coarse block [4]. Coarse grid k^* computed in this manner has been shown to provide accurate solutions to the coarse grid pressure equation. We note that some upscaling procedures additionally introduce a different coarse grid functionality for d, though this does not appear to be essential in our formulation.

In this work, the proposed coarse model is the upscaling of the pressure equation to obtain the velocity field on the coarse grid and use it in saturation equation to resolve the concentration on the coarse grid. We will use multiscale finite element method. The key idea of the method is the construction of basis functions on the coarse grids such that these basis functions capture the small scale information on each of these coarse grids. The method that we use follows its finite element counterpart presented in [9]. The basis functions are constructed from the solution of the leading order homogeneous elliptic equation on each coarse element with some specified boundary conditions. Thus, if we consider a coarse element K that has d vertices, the local basis functions ϕ^i, $i = 1, \ldots, d$, are set to satisfy the following elliptic problem:

$$-\nabla \cdot (k \cdot \nabla \phi^i) = 0 \quad \text{in } K, \quad \phi^i = g^i \quad \text{on } \partial K, \tag{3}$$

for some functions g^i defined on the boundary of the coarse element K. Hou et al. [9] have demonstrated that a careful choice of boundary condition would guarantee the performance of the basis functions to incorporate the local information and, hence improve the accuracy of the method. In this paper, the function g^i for each i varies linearly along ∂K. Thus, for example, in case of a constant diagonal tensor, the solution of (3) would be a standard linear/bilinear basis function. We note that as usual we require $\phi^i(\xi_j) = \delta_{ij}$. Finally, a nodal basis function associated with the vertex ξ in the domain Ω are constructed from the combination of the local basis functions that share this ξ and zero elsewhere. These nodal basis functions are denoted by $\{\psi_\xi\}_{\xi \in Z_h^0}$.

We denote by V^h the space of our approximate pressure solution which is spanned by the basis functions $\{\psi_\xi\}_{\xi \in Z_h^0}$. A statement of mass conservation on a control volume V_ξ is formed from pressure equation, where now the approximate solution is written as a linear combination of the basis functions. To be specific, the problem now is to seek $p^h \in V^h$ with $p^h = \sum_{\xi \in Z_h^0} p_\xi \psi_\xi$ such that

$$\int_{\partial V_\xi} d(S) k \nabla p^h \cdot n \, dl = \int_{V_\xi} q \, dA, \tag{4}$$

for every control volume $V_\xi \subset \Omega$. Here n defines the normal vector on the boundary of the control volume, ∂V_ξ and S is the fine scale saturation field.

For the saturation equation, we will consider two different coarse models. We will present these models based on a perturbation technique, where the saturation, S, and the velocity v, on the fine scale are assumed to be the sum

of their volume-averaged and fluctuating components,

$$v = \overline{v} + v', \quad S = \overline{S} + S', \quad f = \overline{f} + f'. \tag{5}$$

Here the overbar quantities designate the volume average of fine scale quantities over coarse blocks. For simplicity we will assume that the coarse blocks are rectangular which allows us to state that (cf [11]) $\overline{\nabla f} = \nabla \overline{f}$. Substituting (5) into the saturation equation and averaging over coarse blocks we obtain

$$\frac{\partial \overline{S}}{\partial t} + \overline{v} \cdot \nabla \overline{f} + \overline{v' \cdot \nabla f'} = (\tilde{S} - \overline{f})q. \tag{6}$$

The term $\overline{v' \cdot \nabla f'}$ represents subgrid effects due to the heterogeneities of convection.

   The first model is a simple/primitive model where subgrid term $\overline{v' \cdot \nabla f'}$ is ignored:

$$\frac{\partial \overline{S}}{\partial t} + \overline{v} \cdot \nabla f(\overline{S}) = (\tilde{S} - f(\overline{S}))q. \tag{7}$$

This kind of upscaling technique in conjunction with the upscaling of absolute permeability is commonly used in applications (see e.g. [5]). The difference of our approach is that the coupling of the small scales is performed through the finite volume element formulation of the global problem and the small scale information of the velocity field can be easily recovered. Within this upscaling framework we use $\overline{S}$ instead of S in (4). If the saturation profile is smooth this approximation is of first order. In the coarse blocks where the discontinuities of S are present we need to modify the stiffness matrix corresponding to these blocks. The latter requires the values of the fine scale saturation. In our computation we will not do this and simply use $d(\overline{S})$ in (4).

   To improve the primitive upscaled model, one can model the subgrid terms $\overline{v' \cdot \nabla f'}$. First, we briefly review the results for $f(S) = S$ and assume that the perturbations are small. Equation (6) becomes:

$$\frac{\partial \overline{S}}{\partial t} + \overline{v} \cdot \nabla \overline{S} + \overline{v' \cdot \nabla S'} = (\tilde{S} - \overline{S})q. \tag{8}$$

The term $\overline{v' \cdot \nabla S'}$ represents subgrid effects due to the heterogeneities of convection. This term can be modeled using the equation for S' that is derived by subtracting (8) from the fine scale equation

$$\frac{\partial S'}{\partial t} + \overline{v} \cdot \nabla S' + v' \cdot \nabla \overline{S} + v' \cdot \nabla S' = \overline{v' \cdot \nabla S'} - qS'.$$

This equation can be solved along the characteristics $dx/dt = \overline{v}$ by neglecting higher order terms. Carrying out the calculations in an analogous manner to the ones performed in [7] we can easily obtain the following coarse scale saturation equation:

$$\frac{\partial \overline{S}}{\partial t} + \overline{v} \cdot \nabla \overline{S} = \nabla \cdot (D(x,t)\nabla \overline{S}(x,t)) + (\tilde{S} - \overline{S})q, \tag{9}$$

where $D(x,t)$ is the dispersive matrix coefficient, whose entries are written as $D_{ij}(x,t) = \left[\int_0^t \overline{v_i'(x)v_j'(x(\tau))}d\tau\right]$. Next it can be easily shown that the diffusion coefficient can be approximated up to the first order by $D_{ij}(x,t) = \overline{v_i'(x)L_j}$, where L_j is the displacement of the particle in j direction that starts at the point x and travels with velocity $-v$. The diffusion term in the coarse model for the saturation field (9) represents the effects of the small scales on the large ones. Note that the diffusion coefficient is a correlation between the velocity perturbation and the displacement. This is different from [7] where the diffusion is taken to be proportional to the length of the coarse scale trajectory. Using our upscaling methodology for the pressure equation we can recover the small scale features of the velocity field that allows us to compute the fine scale displacement.

For the nonlinear flux $f(S)$ we can use similar argument by expanding $f(S) = f(\overline{S}) + f_S(\overline{S})S' + \cdots$. In this expansion we will take into account only linear terms and assume that the flux is nearly linear. This is similar to the linear case and the analysis can be carried out in an analogous manner. The resulting coarse scale equation has the form

$$\frac{\partial \overline{S}}{\partial t} + \overline{v} \cdot \nabla \overline{S} = \nabla \cdot f_S(\overline{S})^2 D(x,t)\nabla \overline{S}(x,t) + (\tilde{S} - f(\overline{S}))q, \tag{10}$$

where $D(x,t)$ is the macrodiffusion corresponding to the linear flow. This formulation has been derived within stochastic framework in [10]. We note that the higher order terms in the expansion of $f(S)$ may result in other effects which, to our best knowledge, have not been studied extensively. In [6] the authors use similar formulation though their implementation is different from ours.

We now turn our attention to the procedure of computing D_{ij}. Let $L_j(x,t)$, $j = 1,2$, be the trajectory length of the particle in x_j-direction that starts at point x computed as $L_j(x,t) = \int_0^t v_j'(x(\tau),\tau)\,d\tau$. Then $D_{ij}(x,t) \approx \overline{v_i'(x,t)\,L_j(x,t)}$. To show this relation we note

$$D_{ij}(x,t) = \overline{v_i'(x,t)\int_0^t v_j'(x(\tau),\tau)\,d\tau}. \tag{11}$$

We remark that since the velocity depends on (x,t), so is the trajectory in (11), i.e., we have $x(\tau) = r(\tau|x,t)$ with $x(t) = r(t|x,t) = x$. Now let $\tau = t_p < t$. We assume that t_p is close to t. Then we may decompose the time integration in (11) as the sum of two integrations, namely,

$$\int_0^t v_j'(r(\tau|x,t),\tau)\,d\tau = \int_0^{t_p} v_j'(r(\tau|x,t),\tau)\,d\tau + \int_{t_p}^t v_j'(r(\tau|x,t),\tau)\,d\tau = I_1 + I_2.$$

Suppose we denote by y_p the particle location at time t_p. Then $r(\tau|x,t) = r(\tau|y_p, t_p)$, $0 \leq \tau \leq t_p$. Thus, $I_1 = \int_0^{t_p} v_j'(r(\tau|y_p, t_p), \tau) \, d\tau = L_j(y_p, t_p)$. Furthermore, since we have assumed that t_p is close to t, the particle trajectory is still close to x, which gives $I_2 \approx (t - t_p) v_j'(x, t)$. By substituting these representations back to (11) we obtain our macrodispersion, where now we have $L_j(x,t) = L_j(y_p, t_p) + (t - t_p) v_j'(x, t)$. Thus the macrodispersion coefficient may be computed as

$$D_{ij}(x,t) \approx \overline{v_i'(x,t) \, L_j(y_p, t_p)} + (t - t_p) \overline{v_i'(x,t) \, v_j'(x,t)}.$$

This relation also shows us how to numerically compute D_{ij}. We note that the fluctuation components v_i' are obtained by subtracting the average $\overline{v_i}$ from v_i, where v_i is constructed from the informations embedded in the multiscale basis functions. Moreover, since $t_p < t$, $L_j(y_p, t_p)$ has been known. Thus we can compute the macrodispersion coefficients incrementally for each time level. This way, saving velocities information for all time levels may be avoided. The calculation of two-point correlations in spatial framework can produce oscillations. For this reason, the authors in [7] avoid computing two-point correlations and introduce some simplifications. In our simulations, we compute two-point correlation and smooth it to avoid the oscillation. In particular, the obtained macro-dispersion is monotone in time and reaches an asymptote.

3 Numerical Results

In this section we present numerical results that give comparison between the fine and the primitive coarse model, and the coarse model with macrodispersion that accounts for the subgrid effects on the coarse grid. It is expected to see possible improvement on the coarse model performance using this extension. We consider a typical cross section in the subsurface, where the system length in the horizontal direction x (L_x) is greater than the formation thickness (L_z); in the results presented below, $L_x/L_z = 5$. The fine model uses 120×120 rectangular elements. The absolute permeability is set to be $\text{diag}(k, k)$. All of the fine grid permeability fields used in this study are 120×120 realizations of prescribed overall variance (σ^2) and correlation structure. The fields were generated using GSLIB algorithms [3] with a spherical covariance model [3], for which we specify the correlation lengths l_x and l_z, which are normalized by the system length in the corresponding direction. The coarse models use 12×12 elements which is a uniform coarsening of the fine grid description. In the examples presented below, we consider *side to side flow* flow. More precisely, we fix pressure and saturation ($S = 1$) at the inlet edge of the model ($x = 0$) and zero pressure at the outlet ($x = L_x$). The top and bottom boundaries are closed to flow.

We follow the standard practice for solving the two-phase immiscible flow as well as miscible two-component flow which is known as the *implicit pressure*

explicit saturation method. For each time step, the pressure equation is solved first where the dependence of the elliptic equation on the saturation uses the values from the previous time level. The Darcy Law is used to compute the flux. Then the saturation equation is solved explicitly using these computed flux as input. We note that in our upscaled model, the pressure equation is solved by the multiscale finite volume element presented above, while the saturation equation is solved on the coarse grid by standard finite volume difference.

Results are presented in terms of fractional flow of displaced fluid (F, defined as fraction of the displaced fluid in the total produced fluid) versus pore volumes injected (PVI). PVI is analogous to dimensionless time and is defined as qt/V_p where q is the total volumetric flow rate, t is dimensional time and V_p is the total pore volume of the system. Figure 1 shows typical results from multicomponent miscible displacement. It uses an anisotropic field of $l_x = 0.20$, $l_z = 0.02$. In all plots, the solid line represents the fine model run on 120×120 elements which serves as a reference solution. The dashed line represents the primitive coarse model ($D = 0$), while the dotted line represents the coarse model with macrodispersion (with D). All coarse models are run on the 12×12 elements. In this figure we show how the performance of our coarse model varies with respect to the mobility ratio, M, and the overall variance of the permeability, σ. The left plot corresponds to the coarse model using $M = 2$ and $\sigma = 1.5$, the right plot corresponds to $M = 5$ and $\sigma = 1.5$. In all these cases we see that the addition of the macrodispersion to our coarse model improves the prediction of the breakthrough. Similar improvement has been observed in two-phase immiscible flow as well as in saturation contours. Due to page limitation, we do not include these results in the paper.
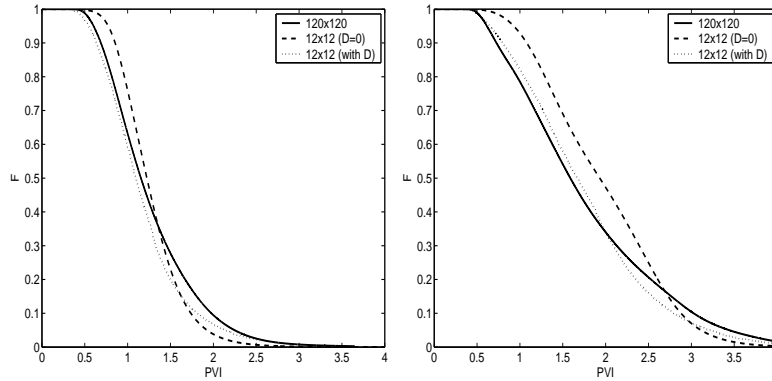

Fig. 1. Comparison of fractional flow of displaced fluid at the production edge for side to side flow. All coarse models are run on 12×12 elements. The permeability has correlation lengths $l_x = 0.20$, $l_z = 0.02$. Left: $M = 2$, $\sigma = 1.5$, Right: $M = 5$, $\sigma = 1.5$.

Summarizing the results, we see that the correction to primitive upscaled saturation equation using perturbation techniques gives an improvement. When the flux, $f(S)$, is a linear function, we do not need to perform linearization of the fluxes and the errors are only due to perturbations of the velocity field. The latter can be controlled by choosing adaptive grid or using adaptive coordinate system. In particular, our results presented in [8] show that in pressure-streamline coordinate system, perturbation techniques work better because the grid is adapted to the flow. In the presence of sharp fronts, one can use subgrid models away from these fronts and follow the front dynamics separately. This approach is also implemented in [8] in pressure-streamline coordinate system and we have observed further improvement in the performance of the method.

References

[1] M.A. Christie. Upscaling for reservoir simulation. *J. Pet. Tech.*, pages 1004–1010, 1996.

[2] N.H. Darman, G.E. Pickup, and K.S. Sorbie. A comparison of two-phase dynamic upscaling methods based on fluid potentials. *Comput. Geosci.*, 6:5–27, 2002.

[3] C.V. Deutsch and A.G. Journel. *GSLIB: Geostatistical Software Library and User's Guide*. Oxford University Press, New York, 2nd edition, 1998.

[4] L.J. Durlofsky. Numerical calculation of equivalent grid block permeability tensors for heterogeneous porous media. *Water Resour. Res.*, 27:699–708, 1991.

[5] L.J. Durlofsky, R.C. Jones, and W.J. Milliken. A nonuniform coarsening approach for the scale up of displacement processes in heterogeneous media. *Adv. in Water Res.*, 20:335–347, 1997.

[6] Y.R. Efendiev and L.J. Durlofsky. Numerical modeling of subgrid heterogeneity in two phase flow simulations. *Water Resour. Res.*, 38(8):1128, 2002.

[7] Y.R. Efendiev, L.J. Durlofsky, and S.H. Lee. Modeling of subgrid effects in coarse scale simulations of transport in heterogeneous porous media. *Water Resour. Res.*, 36:2031–2041, 2000.

[8] Y.R. Efendiev, T.Y. Hou, and T. Strinopoulos. Multiscale simulations of porous media flows in flow-based coordinate. *Comput. Geosci.*, 2006. submitted.

[9] T.Y. Hou and X.H. Wu. A multiscale finite element method for elliptic problems in composite materials and porous media. *J. Comput. Phys.*, 134:169–189, 1997.

[10] P. Langlo and M.S. Espedal. Macrodispersion for two-phase, immisible flow in porous media. *Adv. in Water Res.*, 17:297–316, 1994.

[11] W. Zijl and A. Trykozko. Numerical homogenization of two-phase flow in porous media. *Comput. Geosci.*, 6(1):49–71, 2002.